

Growth evolution of ZnO thin films deposited by RF magnetron sputtering

This article has been downloaded from IOPscience. Please scroll down to see the full text article.

2012 J. Phys.: Conf. Ser. 370 012020

(<http://iopscience.iop.org/1742-6596/370/1/012020>)

View [the table of contents for this issue](#), or go to the [journal homepage](#) for more

Download details:

IP Address: 200.145.3.40

The article was downloaded on 18/07/2013 at 21:10

Please note that [terms and conditions apply](#).

Growth evolution of ZnO thin films deposited by RF magnetron sputtering

A M Rosa¹, E P da Silva¹, E Amorim¹, M Chaves¹, A C Catto², P N Lisboa-Filho²
and J R R Bortoleto¹

¹ Laboratory of Technological Plasmas, São Paulo State University-UNESP,
Av. 3 de Março, 511, Sorocaba, Brazil

² Grupo de Materiais Avançados, São Paulo State University-UNESP,
Av. Eng. Luiz Edmundo Carrijo Coube, 14-01, Bauru, Brazil

E-mail: dre_rosa_16@hotmail.com

Abstract. We study the surface morphology evolution of ZnO thin films grown on glass substrates as a function of thickness by RF magnetron sputtering technique. The surface topography of the samples is measured by atomic force microscopy (AFM). All AFM images of the films are analyzed using scaling concepts. The results show that the surface morphology is initially formed by a small grains structure. The grains increase in size and height with growth time resulting in the formation of a mounds-like structure. The growth exponent, β , and the exponent defining the evolution of the characteristic wavelength of the surface, p , amounted to $\beta = 0.76 \pm 0.08$ and $p = 0.3 \pm 0.05$. From these exponents, the surface morphology is determined by the nonlocal shadowing effects, that is the dominant mechanism, due to the incident deposition particles during film growth.

1. Introduction

Zinc oxide (ZnO) has gained much attention due to its versatile nature. Actually, ZnO is a wide band gap semiconductor (3.37 eV at room temperature) that can be used in numerous applications such as solar cells [1], flat displays, heat mirrors, TFTs and chemical sensors [2]. In particular, it is a promising alternative to indium tin oxide (ITO) in transparent conducting oxide (TCO) applications, due to its low cost, non-toxicity and the stability under hydrogen plasma [2,3]. ZnO thin films have been synthesized by a wide variety of techniques including chemical and physical routes, such as pulsed laser deposition [4], thermal evaporation [5], chemical vapor deposition [6,7], electron beam evaporation [5], spray pyrolysis [8], sol-gel method [9] and magnetron sputtering on a variety of substrates [10,11]. The advantages of magnetron sputtering are high deposition rate, low substrate temperature, good adhesion of the film to the substrate and the simple apparatus [10].

In thin film growth, the morphologies of growth fronts and their evolution reflect the microscopic growth dynamics. Under the common conditions, the growth of thin films is a process of far from-equilibrium that can lead to the evolution of nanostructures on front surfaces [12]. Thus, many of the properties of thin films, from the point of view of the applications, depend on their surface properties, particularly on the surface roughness [4,12,13].

The knowledge of the mechanisms that determine the thin film morphological evolution has motivated a large volume of research last years. A great emphasis has been given to the theoretical and

experimental study of thin film growth evolution [14]. Two typical lengths are still employed to study the growth dynamics [15]: the surface roughness, σ (the rms height fluctuation around the mean height value) and the lateral correlation length, ξ , is linked with the characteristic distance between mounds on the surface. It is assumed that σ and ξ evolves with growth time, t , as $\sigma \sim t^\beta$ and $\xi \sim t^p$, respectively [15]. The exponent β is known as the growth exponent and p is known as the exponent defining the evolution of the characteristic wavelength of the surface [12,14,16]. These exponents depend on the growth mechanisms operating during deposition, which resulting the film structure [4].

In this paper, we investigate the growth dynamics of ZnO thin films via the RF magnetron sputtering technique. This research consist the determination of the growth regime of the thin film through the analysis of the exponents scaling. Thus, the experimental determination of the values of the exponents β and p and their comparisons with the existing values of the literature allow identifying the main growth mechanisms involved in the film deposition.

2. Experiment

The experimental setup used in this work consists of a cylindrical stainless steel chamber, with 330 mm diameter and 200 mm high. Inside the reactor there are two stainless steel circular plates (electrodes) with 100 mm diameter, separated by distance of 50 mm. Gases were controlled through needle valves (Edwards, model LV-10K) and by flow meter and pressure was monitored by Pirani gauge. The system was evacuated by a vacuum rotary vane pump (Leybold D25B) lowering pressure to 1.0×10^{-3} Torr. The plasma was activated by coupling a source of RF (13.56 MHz, 300W with impedance matching Tokyo Hy-Power Labs) capacitively coupled to the internal electrodes of the chamber.

ZnO films were deposited on $10 \times 30 \times 3$ mm³ rectangular glass substrates by RF magnetron sputtering technique. The glass substrates were ultrasonically cleaned in detergent diluted in deionized water, rinsed in new ultrasonic bath in deionized water and a final ultrasonic bath in isopropyl alcohol. Afterwards, the substrates were dried in a hot air flow and positioned in the sample holder (top electrode). A metallic zinc target with 50 mm diameter and 99.99% purity was used as zinc source. The plasma was activated by a 13.56 MHz RF power of 70 W in argon pressure of 1.0×10^{-2} Torr and flow of oxygen of 0.10 sccm. In the lower electrode was mounted a set of magnets of Samarium-Cobalt (SmCo), with circular geometry, and on top of the set of magnets was placed the metallic zinc target. In the top electrode was placed the glass substrate and this was grounded while the lower electrode was applied of RF power. The substrate temperature was measured after the deposition by a thermocouple and it was maintained around 353 K. The ZnO thin film growth rate was approximately 5 nm/ min. In order to study the growth evolution, different ZnO films with thickness ranging from 0 up to 547 nm were deposited.

The thickness was measured in a profilometer Veeco Dektak 150. Surface morphology was measured with atomic force microscopy (AFM, XE-100, Park Systems) operating in non-contact mode. Silicon cantilevers were employed (nominal radius of 10 nm). The scan area was $1 \mu\text{m} \times 1 \mu\text{m}$ with a resolution of 512×512 pixels. The AFM images were acquired; the surface roughness was characterized in terms of root mean square roughness (RMS), σ , and lateral correlation length, ξ .

The parameters σ and ξ are obtained from the surface morphology measured by AFM. σ is mathematically defined by equation [17]:

$$\sigma = \sqrt{\frac{1}{N} \sum_{i=1}^N (h_i - \bar{h})^2} \quad (1)$$

The value of σ was obtained directly from the $1 \mu\text{m} \times 1 \mu\text{m}$ AFM images using the software XEI (Park Systems). The lateral correlation length ξ is related to the characteristic distance between mounds on the surface. The average value of ξ was calculated from a Lorentz fitting of the power spectral density (PSD) calculated from $1 \mu\text{m} \times 1 \mu\text{m}$ AFM images. The PSD curves are provided by software XEI. The peak of the PSD curves for each thickness was used to select the wavelength λ on the surface. The

average value of ξ was considered the inverse of λ , $\xi = 1/\lambda$. These measurements were used to determine the growth exponent β and the exponent defining the evolution of the characteristic wavelength of the surface p . These exponents were derived fitting in graphics of roughness and correlation length, respectively. The crystalline degree and crystal orientation of ZnO thin films was measured using an x-ray diffractometer system (D/MAX-2100/PC, Rigaku) in grazing incidence geometry. X-ray diffraction patterns confirm the proper phase formation of the material.

3. Results and discussion

Figure 1 shows AFM images of the ZnO thin films grown on glass substrate as a function of thicknesses. The surface morphology is mainly formed by small grains. As the deposition goes further increases the density of large structure, which grows continuously in lateral size and height, tends to exhibit mounds-like structure. As shown AFM images in figure 1, the grain size spatial distribution is very homogeneous for all films. Vasco et al. [4] reported the presence of two growth regimes for ZnO/InP(100) films grown by PLD technique. Similar behavior is found in the first regime in which the surface morphology is mainly formed by a granular structure as well. In second regime, there are an increase of the large structure, which grows both in width and height, tending to display a stepped pyramid-like structure.

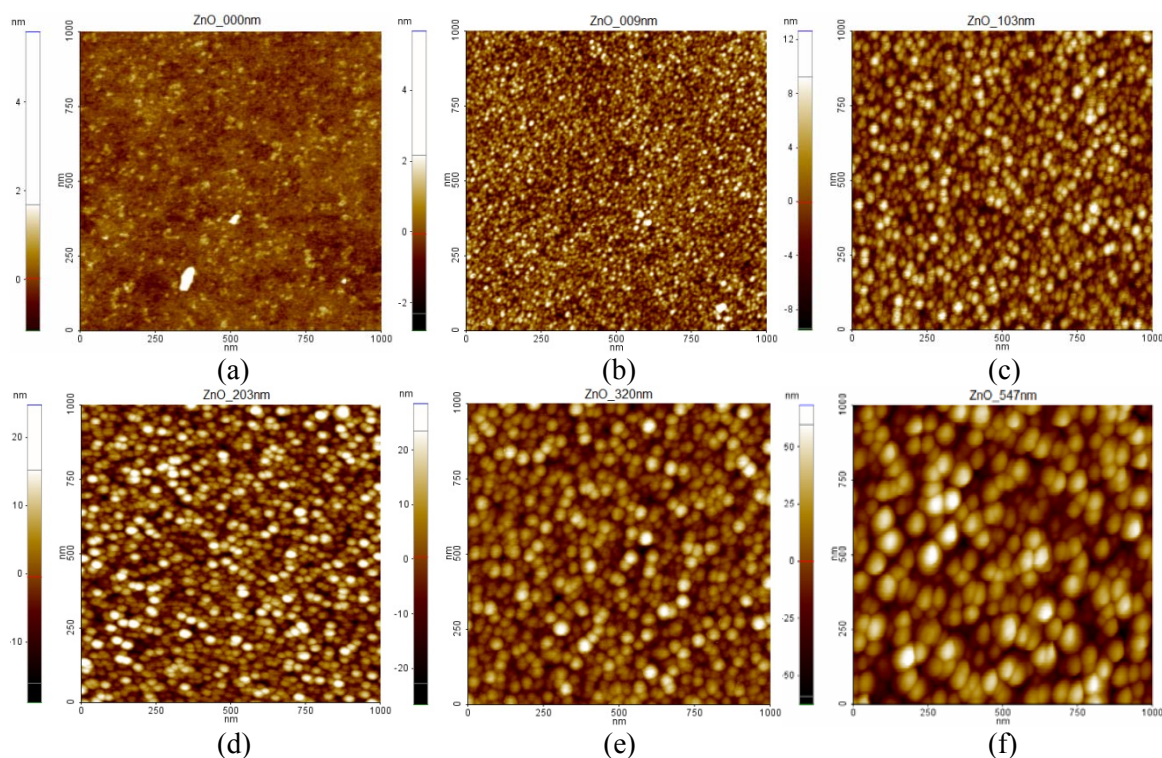


Figure 1. $1\ \mu\text{m} \times 1\ \mu\text{m}$ AFM images of glass substrate and ZnO thin films with different thickness. (a) glass substrate, (b) 9 nm, (c) 103 nm, (d) 203 nm, (e) 320 nm and (f) 547 nm.

Figure 2 shows the profile height of the surface topography of the (a) glass substrate and ZnO thin films with (b) 203 and (c) 547 nm thick along the fast scan direction. The growth evolution of the granular structures and the formation of mound-like structure are evident. From figure 2 a rough surface is apparent, i.e., the increase along of vertical direction of surface irregularities. The same behavior has been reported by Fu and Shen for thin Al/Si(100) [16] films sputter-deposited. They reported the increase of mounds in size and height with growth time.

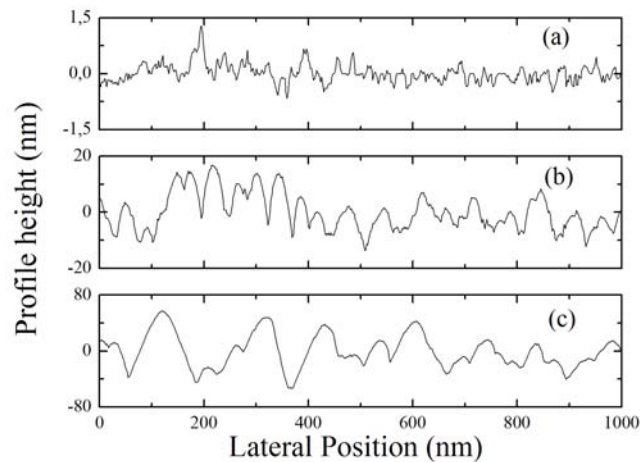


Figure 2. Surfaces profiles taken from $1\ \mu\text{m}\times 1\ \mu\text{m}$ AFM images of glass substrate and ZnO thin films. (a) glass substrate, (b) 203 nm thick with $\xi = 79.5\ \text{nm}$ and (c) 547 nm thick with $\xi = 179\ \text{nm}$.

In figure 3 it is shown the evolution of σ with films thicknesses and the calculation of exponent β . From the measurements of AFM images is determined the σ data. The growth exponent β is calculated from the slope of the log-log representation of the surface roughness as a function of thickness. By fitting the roughness data, the $\beta = 0.76 \pm 0.08$ while Vasco et al. [4] and Álvarez et al [12] reported $\beta = 1.0 \pm 0.1$ and Fu and Shen [16] related $\beta = 0.56 \pm 0.03$. So, the process of film growth is characterized by a growth unstable, i.e., $\beta \geq 0.5$ [14]. The growth of structures along the vertical direction is faster for larger β value, i.e., for the films ZnO/InP(100) [4] and ZrO₂ [12] compared with our films.

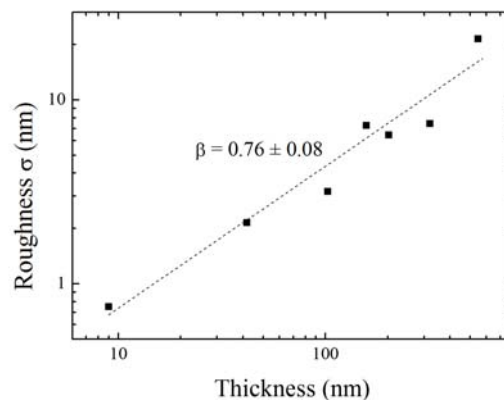


Figure 3. The roughness surface evolution with the ZnO films thicknesses as measured on $1\ \mu\text{m}\times 1\ \mu\text{m}$ AFM images and the calculation of the exponent β for the films grown. The dash line is the best fit obtained for the calculation.

Figure 4 shows the evolution of ξ with film thicknesses. The lateral correlation length ξ is derived from the peaks λ of the 2D power spectrum density (PSD) of the AFM images of the grown films, i.e., $\xi = 1/\lambda$. The p is calculated from the slope of the log-log representation of the lateral correlation length as a function of thickness. By fitting of the ξ data, $p = 0.30 \pm 0.05$ while Vasco et al. [4] $p =$

0.33 ± 0.05 , Álvarez et al. [12] $p = 0.34 \pm 0.03$ and Fu and Shen [16] reported $p = 0.36$. In a simplified way, AFM data show that ξ evolves from 43 up to 179 nm with film thickness.

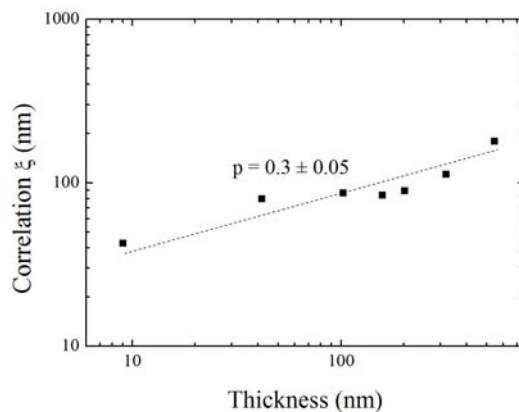


Figure 4. The correlation length ξ evolution as calculated from a Lorentz fitting of 2D power spectrum density of $1 \mu\text{m} \times 1 \mu\text{m}$ AFM images. The calculation of the exponent p for the grown films and the dash line is the best fit obtained.

Figure 5 displays (a) the x-ray diffraction pattern, and (b) correlation length ξ , solid square, and grain size, empty triangle, for ZnO films with different thicknesses. In the spectrum of figure 5(a) is possible to observe increasing the intensity of the (002) and (201) peaks with thickness. No peak is observed in ZnO film with 9 nm thick, because it is very thin it is impossible to detect the diffraction peaks. The presence of the (100), (002) and (201) peaks in ZnO film with 547 nm thick indicates that it is a polycrystal, this fact is less evident in smaller thicknesses. A strong (002) peak can be seen with a preferential orientation along c-axis perpendicular to the substrate surface according to the literature [18]. Lin et al. [10] reported that ZnO film deposited with thickness below 500 nm were polycrystalline with a c-axis preferential orientation. This preferential orientation in sputtered ZnO films is due to the lowest surface free energy of (002) plane according to Fujimura et al. [19].

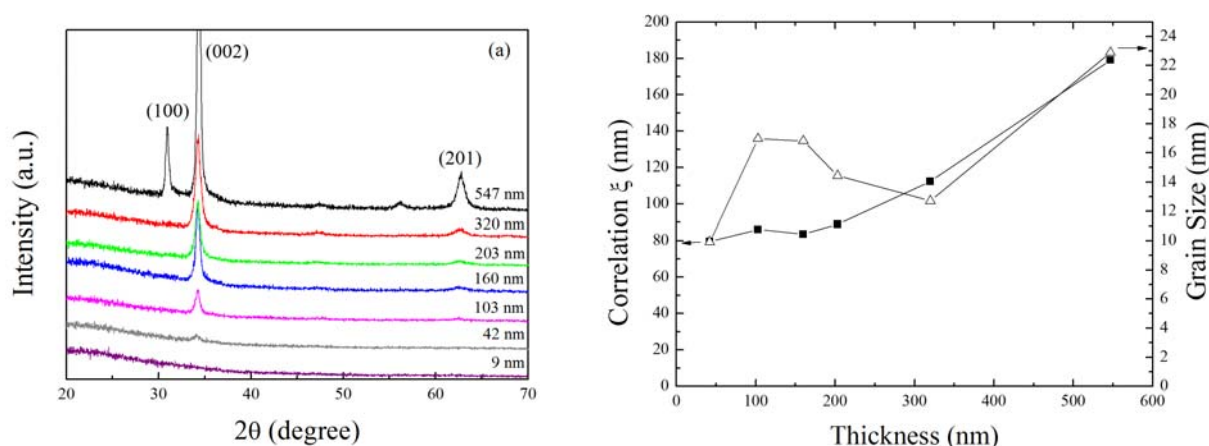


Figure 5. (a) The x-ray diffraction pattern of ZnO films and (b) correlation length ξ (solid square) and the grain size (empty triangle) for ZnO films with different thicknesses.

Figure 5(b) shows similar behavior of correlation ξ and size grain that tend to increase as a function of thicknesses. The grain size of ZnO films is calculated using Scherrer's formula [10,20]:

$$D = \frac{0.9\lambda}{\beta \cos \theta} \quad (2)$$

where $\lambda = 1.54 \text{ \AA}$, β the value FWHM in radians and θ Bragg angle. The grain size increased with the increase of film thickness. The film with 203 nm thick has about 14 nm of grain size and 79.5 nm of ξ while the film thickness of 547 nm is observed about 23 nm and 179 nm of ξ . It is clear in figures 2(b) and 2(c) that shown surfaces profiles of ZnO films.

The formation of mounds-like structures on the surface of ZnO films is related to the dynamic growth far from equilibrium ($\beta \geq 0.5$) and to nonlocal effects. The nonlocal effects are growth mechanisms that during the deposition affect the film morphology evolution such as step-edge barriers, the shadowing, diffusional instability, sputtering, etc. [4,12,16]. Among them, two mechanisms must be taken into account: the shadowing of incident deposition particles, which becomes important when random incidence, and the diffusion mechanism tends to smooth a growing surface [12,14,21].

The shadowing has a strong effect on the formation of a mounds-like structure [14]. This occurs due to the vapor atoms, that incoming from all directions, stick where are first deposited [14,21]. The grass model illustrates nicely the effect of shadowing [14,21]. In this model, the growth of each "blade of grass" is related to the amount of light arriving at their tips. The initial configuration is blades of grass with small but random differences in heights. The shortest are shadowed by their taller neighbors, and stop growing. This also happens during the deposition when the valleys are shadowed by the peaks. This creates instability in the growth of the film that leads to the increases of the structures along the vertical direction causing the roughness. As a competing mechanism, diffusion erodes peaks and fills in the valleys, i.e., creates a more energetically stable structure [12,21]

By considering the experimental results obtained for the ZnO thin films grown on glass substrates is possible to identify the dominant growth mechanism that operates during deposition. The growth exponent $\beta = 0.76$ is found in our work while Vasco et al. [4] and Álvarez et al. [12] found a higher β value, $\beta = 1.0$. They related that the dominant mechanism is the shadowing. Sometimes it is not possible to identify the dominant mechanism as reported by Fu and Shen [16]. They related that the nonlocal shadowing effect work together with diffusion mechanism in the film growth resulting in a lower β value, $\beta = 0.56$. From these results it can be concluded that the growth dynamic behavior observed when the mounds-like structures developed is consistent with that expected when shadowing effects determine the growth mode. This behavior is consistent with the images of AFM in the figure 1 that show the development both in lateral size and height of the small grains as a function of thicknesses. Together with shadowing effect, diffusion mechanism is present in the growth dynamic, but at a lower magnitude. It must be noted that the shadowing effects dominates over diffusion mechanism.

4. Conclusions

In conclusion, it has been observed that ZnO thin films grown on glass substrates by RF magnetron sputtering technique show that the surface morphology is initially formed by small grains. As the deposition goes further increases the grains both lateral size and height resulting in the formation of a mounds-like structure. We have determined the exponents that characterize the dynamic growth and found that $\beta = 0.76 \pm 0.08$ and $p = 0.30 \pm 0.05$. From these results compared with the existing values in the literature can be concluded that the mechanism dominant in the surface morphology evolution is the nonlocal shadowing effects. However, together with shadowing effect, the diffusion mechanism acts in the growth dynamic at a lower magnitude. The growth behavior observed for the mounds-like structure is consistent with the existence of nonlocal shadowing effects.

Acknowledgments

The financial support from Fapesp and CNPq are gratefully acknowledged.

References

- [1] Li Y L, Lee D Y, Min S R, Cho H N, Kim J S and Chung C W 2008 *Japan. J. Appl. Phys.* **47** 6896
- [2] Lee S, Bang S, Park J, Park S, Jeong W and Jeon H 2010 *Phys. Status Solidi* **207** 1845-9
- [3] Jiang M, Liu X and Wang H 2009 *Surface & Coatings Technology* **203** 3750-3
- [4] Vasco E, Zaldo C and Vázquez L 2001 *J. Phys.: Condens. Matter* **13** L663-72
- [5] Mtangi W., Auret F D, Janse van Rensburg P J, Coelho S M M, Legodi M J et al. 2011 *J. Appl. Phys.* **100** 094504
- [6] Kasuga M and Ishihara S 1976 *Japan. J. Appl. Phys.* **15** 1835
- [7] Choi Y S, Hwang D K, Kwon B J, Kang J W, Cho Y H and Park S J 2011 *Japan. J. Appl. Phys.* **50** 10550
- [8] Sonmez E, Aydin S, Yilmaz M, Yurtcan M T, Karacali T and Ertugrul M 2012 *Journal of Nanomaterials* **2012** 950793
- [9] Mamata M H, Khusaimib Z, Musaa M Z, Maleka M F and Rusopa M 2011 *Sensor and Actuators A* **171** 241-7
- [10] Lin S-S and Huang J-H 2004 *Surface & Coatings Technology* **185** 222-07
- [11] Shin J W, No Y S, Lee J Y, Kim J Y, Choi W K and Kim T W 2011 *Appl. Surf. Sci.* **257** 7516-20
- [12] Álvarez R, Palmero A, Pietro-López L O, Yubero F, Cotrino J and Cruz W 2010 *J. Appl. Phys.* **107** 54311
- [13] Liu Y, Yang S, Wei G, Song H, Cheng C, Xué C and Yuan Y 2011 *Surface & Coatings Technology* **205** 3530-4
- [14] Barabási A L and Stanley H E 1995 *Fractal Concepts in Surface Growth* (Cambridge: Cambridge University Press)
- [15] Smilauer P and Vvedensky D 1995 *Phys. Rev. B* **52** 14263
- [16] Fu T and Shen Y G 2008 *Phys. B* **403** 2306-11
- [17] Gadelmawala E S, Koura M M, Maksound T M, Elewa I M and Soliman H H 2002 *Journal of Materials Processing Technology* **123** 133-45
- [18] Rolo A G, Campos J A, Viseu T, Arôso T L and Cerqueira M F 2007 *Superlattices and Microstructures*. **42** 265-009
- [19] Fujimura N, Nishihara T, Goto S, Xu J and Ito T 1993 *J. Cryst. Growth* **130** 269
- [20] Ramana C V, Vemuri R S, Fernandez I and Campbell A L 2009 *Appl. Phys. Lett.* **95** 231905
- [21] Karunasiri R P U, Bruinsma R and Rudnick J 1989 *Physical Review Letters* **62** 788-91